BMC Biotechnology

RESEARCH Open Access

The effect of plasma activated water on antimicrobial activity of silver nanoparticles biosynthesized by cyanobacterium *Alborzia kermanshahica*

Bahareh Nowruzi[1*], Hassan Beiranvand[1], Fatemeh Malihi Aghdam[1] and Rojan Barandak[1]

Abstract

Background Silver nanoparticles are extensively researched for their antimicrobial properties. Cold atmospheric plasma, containing reactive oxygen and nitrogen species, is increasingly used for disinfecting microbes, wound healing, and cancer treatment. Therefore, this study examined the effect of water activated by dielectric barrier discharge (DBD) plasma and gliding arc discharge plasma on the antimicrobial activity of silver nanoparticles from *Alborzia kermanshahica*.

Methods Silver nanoparticles were synthesized using the boiling method, as well as biomass from *Alborzia kermanshahica* extract grown in water activated by DBD and GA plasma. The physicochemical properties of the synthesized nanoparticles were evaluated using UV-vis spectroscopy, Fourier-transform infrared (FTIR) spectroscopy, dynamic light scattering (DLS), zeta potential analysis, transmission electron microscopy (TEM), and gas chromatography-mass spectrometry (GC-MS) analysis. Additionally, the disk diffusion method was used to assess the antimicrobial efficacy of the manufactured nanoparticles against both Gram-positive and Gram-negative bacteria.

Results The spectroscopy results verified the presence of silver nanoparticles, indicating their biosynthesis. The highest amount of absorption (1.049) belonged to the nanoparticles synthesized by boiling under GA plasma conditions. Comparing the FTIR spectra of the plasma-treated samples with DBD and GA revealed that the DBD-treated samples had more intense peaks, indicating that the DBD method proved to be more effective in enhancing the functional groups on the silver nanoparticles. The DLS results revealed that the boiling method synthesized silver nanoparticles under DBD plasma treatment had a smaller particle size (149.89 nm) with a PDI of 0.251 compared to the GA method, and the DBD method produced nanoparticles with a higher zeta potential (27.7 mV) than the GA method, indicating greater stability of the biosynthesized nanoparticles. Moreover, the highest antimicrobial properties against *E. coli* (14.333 ± 0.47 mm) were found in the DBD-treated nanoparticles. TEM tests confirmed that spherical nanoparticles attacked the E. coli bacterial membrane, causing cell membrane destruction and cell death. The GC-MS results showed that compounds like 2-methylfuran, 3-methylbutanal, 2-methylbutanal, 3-hydroxy-2-

*Correspondence:
Bahareh Nowruzi
bahareh.nowruzi@srbiau.ac.ir

Full list of author information is available at the end of the article

butanone, benzaldehyde, 2-phenylethanol, and 3-octen-2-ol were much higher in the samples that were treated with DBD compared to the samples that were treated with GA plasma.

Conclusion The research indicated that DBD plasma was more efficient than GA plasma in boosting the antimicrobial characteristics of nanoparticles. These results might be a cornerstone for future advancements in utilizing cold plasma to create nanoparticles with enhanced antimicrobial properties.

Keywords Silver nanoparticles, Dielectric barrier discharge plasma, Gliding arc plasma, Cyanobacteria *Alborzia kermanshahica*

Introduction

Cyanobacteria are photoautotrophic prokaryotes found in various ecosystems that can fix atmospheric nitrogen through nitrogen reduction enzymes [1]. They play a crucial role in the biotransformation of metals to nanoparticles, removing heavy metal ions. They contain biomolecules like secondary metabolites, proteins, enzymes, and pigments, which have antimicrobial and anticancer properties. Their high growth rate promotes biomass production, making them important nanotechnology-mediated microorganisms for nanobiofactories [2, 3].

NP synthesis involves various methodologies, including conventional chemical and physical approaches, as well as modern biological synthesis using natural organisms, enzymes, and vitamins [4]. Few studies have utilized cyanobacteria as the biological machinery for NP fabrication, despite numerous reports of biological synthesis using plants, algae, bacteria, and fungi. Cyanobacteria are crucial biofactories for synthesizing nanoparticles due to their ease of culture, high growth rate, variable biocompounds, heavy metal ion absorption capacity, and environmental safety. Different strains can form various types of nanoparticles, including metallic, metal oxide, Ag-Au nanoalloys, and semiconductor nanoparticles like CdS NPs. These strains can also form other nanomaterials and semiconductor nanoparticles [5–9].

Silver-NPs are widely used metal nanoparticles in various industries, including dressings, surgical instruments, detergents, and care products [10–13]. Traditionally, Ag-NPs were fabricated using chemical and physical methods, but due to high costs, energy requirements, and toxic byproducts, green synthesis methods have been developed to produce clean NPs [14, 15].

Cyanobacteria-mediated nanoparticles exhibit diverse biological, physical, and chemical properties, enabling a wide range of applications. Numerous studies indicate that these nanoparticles can function as antimicrobial, anticancer, and photocatalytic agents, among other applications. Cyanobacterial strains, including *Desertifilum* sp. and *Nostoc* sp., have been evaluated for their ability to synthesize silver nanoparticles (Ag-NPs) that exhibit notable anticancer activity against diverse cancer cell lines [4, 16]. Additionally, Ag-NPs and Au-NPs synthesized from Spirulina sp. and Anabaena sp. exhibit broad-spectrum inhibitory effects against both Gram-positive and Gram-negative bacteria [17–19].

Plasma is a quasi-neutral system created in an electromagnetic field by the flow of neutral gases like helium, argon, nitrogen, oxygen, or atmospheric air [20]. It contains a mixture of radicals, ultraviolet radiation, charged particles, exited metastable atoms, and electric fields. Plasma can be categorized into three types: low-pressure, atmospheric-pressure, and high-pressure plasma, and can be further divided into thermal and non-thermal (cold) plasma [21]. Cold plasma contains complex chemical compounds that work together to inhibit microbial activity. Factors like gas composition, flow rate, humidity, temperature, voltage, frequency, and device design influence its composition and effectiveness [22, 23]. Various gases can be used to generate cold plasma through methods like dielectric barrier discharge, plasma jet, corona discharge, and gliding arc discharge [24–26].

Cold plasma inactivates bacteria through the use of reactive oxygen species (ROS), reactive neutrons (RNS), UV radiation, and charged particles. ROS like ozone, atomic oxygen, singlet oxygen, superoxide, peroxide, and hydroxyl radicals are particularly effective in inhibiting bacterial activity, particularly in anaerobic bacteria, which can potentially damage the cytoplasmic membrane, DNA, and proteins [27–30].

Cold plasma (CP) has garnered significant attention as an innovative technique for nanoparticle production [31]. The reduction of metal ions at the gas-liquid interface can be initiated by electrons, which possess energies up to several electron volts, generated by atmospheric pressure plasma [32]. Nanoparticles can be synthesized through various types of plasma [33]: (a) direct plasma, which involves a gas discharge between electrodes, and (b) remote plasma or plasma jet, characterized by a gas discharge between an electrode and the electrolyte surface. Plasma frequently functions as the cathode [34]. Atmospheric pressure plasma functioning at room temperature has garnered significant attention owing to its scalability, cost-effectiveness, and compact dimensions [35, 36].

The unicellular strain *Alborzia kermanshahica* was isolated from agricultural fields in Kermanshah province

and is classified within the order Chroococcales. Nowruzi and Soares (2021) identified and documented the toxic genes of the strain responsible for microcystin production [37].

The development and enhancement of biosynthetic processes utilizing cyanobacteria, combined with the advantageous characteristics of cold plasma technology—such as cost-effectiveness and environmental sustainability—may facilitate the discovery of novel biogenic nanoparticles with distinctive properties for diverse applications.

The application of cold plasma technology for the production of nanoparticles with enhanced properties (especially antimicrobial activity against harmful bacteria both Gram-positive and Gram-negative) from an Iranian cyanobacterium strain may serve as an alternative to numerous chemical antibiotics presently available in the market. The rise of bacteria resistant to commercial antibiotics underscores the importance of discovering and introducing new antibiotic sources, which has substantial implications for biomedical science. The application of this technology is crucial for improving the antimicrobial properties of cyanobacterium nanoparticles, which may aid in the prevention and treatment of various diseases.

Research on cold plasma and nanoparticle production has been conducted, as previously discussed [31]. However, no studies have been conducted on the use of activated water and biomass from cyanobacterial species in conjunction with cold plasma for the synthesis of nanoparticles to date. Hence, the purpose of this research was the application of atmospheric cold plasma in the ability of this native Iranian cyanobacterium *Alborzia kermanshahica* to produce silver nanoparticles and also the antibacterial properties of the synthesized silver nanoparticles.

Materials and methods

Cyanobacterium strain culture

The cyanobacterium strain *Alborzia kermanshahica* was cultured from the cyanobacteria culture collection (CCC) at Islamic Azad University, Science and Research Branch, and it was confirmed that the cultures were pure and axenic (free from other organisms). The purified samples were cultured in Z8 liquid medium in a growth chamber at a temperature of 28±2 °C with continuous fluorescent lighting at an intensity of 300 μE/m²/s. After 14 days, the cultures containing *Alborzia kermanshahica* were centrifuged. The resulting biomass was then cultured again in Z8 medium containing plasma-activated water and distilled water [38].

Production of plasma activated water (PAW)

The dielectric barrier discharge (DBD) plasma and gliding arc discharge plasma (Phenix BK130/3 AC Test Set 600 Series Processor, Phenix Technologies, USA) was used by a portable surface discharge device to generate plasma. In this study we used two different types of plasma to increase the antimicrobial properties of nanoparticles, and we separately compared each type's performance to choose a more effective method (Fig. 1).

The dielectric barrier discharge (DBD) plasma gadget was powered by a 12 V direct current (DC) battery, which is converted to alternating current (AC) at a voltage of 220 V using an inverter. The device is linked to a high-voltage module designed for amplification. It incorporates a high-voltage electrode composed of stainless steel. To facilitate the generation of plasma along the surface discharge, a PTFE dielectric plate was used, powered by a battery. The gadget exhibits a discharge voltage of 20 kV and operates at a frequency of 18 kHz at 15 (P_{15}) minutes for both activated water and biomass samples [39].

A laboratory-scale gliding arc discharge plasma reactor was constructed using two copper electrodes, each with a thickness of 1.5 mm, a length of 10.4 cm, and a gap distance of 0.5 cm. The energy necessary for ionizing the city gas between the two electrodes within the plasma nozzle is supplied by a power source that generates pulses with a peak voltage of 10 kV, a frequency of 20 kHz, and an average output power of 700 watts. Air was directed into the nozzle at a constant rate of 35 L per minute via an air flow controller, resulting in a uniform plasma flow produced by a strong electric field at high frequencies. Both activated water and biomass samples were subjected to plasma conditions for 15 min [40].

Silver nanoparticle synthesis using biomass method

The cyanobacteria cultures, grown for 14 days in the logarithmic phase (using either atmospheric plasma-activated water or distilled water), were separated by centrifugation at 5000 rpm for 10 min at 20 °C. The specimens underwent three rounds of washing with distilled water. Next, 1 gram of wet biomass was added to 500 ml flasks that already had 100 ml of silver nitrate solution with concentrations of 1, 2, and 3 mM made with distilled water. The mixture was then stirred until the pH reached 7. In the process of synthesis, a shift in color from green to brown was noted, suggesting the creation of silver nanoparticles [41].

The inoculated mixtures were continuously shaken at a temperature of 28 to 30 °C. Samples were taken at 0, 12, 24, 48, and 72-h intervals. For each sample, 1 ml of the solution was removed, centrifuged at 4000 rpm for 1 min, and then analyzed by spectrophotometry with a resolution of 1 nm in the range of 300 to 800 nm. Peaks in the 400 to 450 nm range were considered to indicate the presence of produced nanoparticles [42].

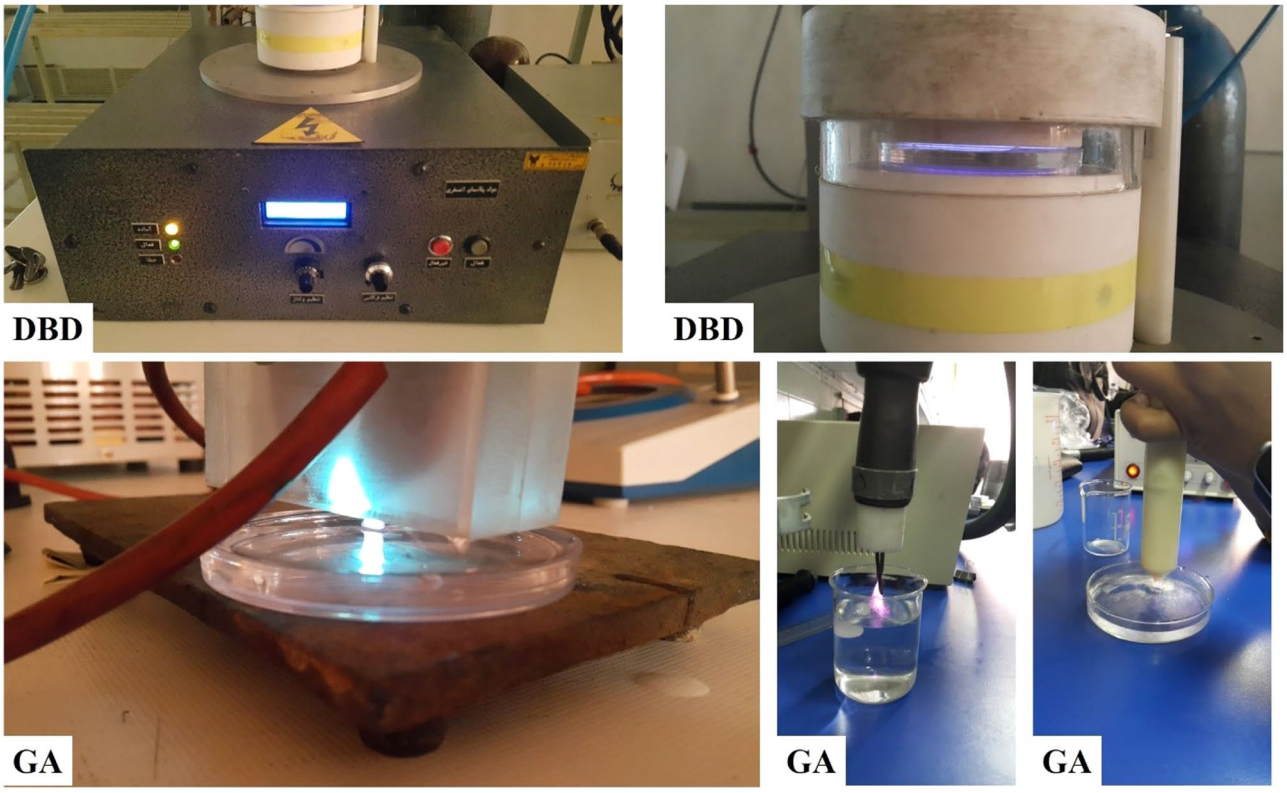

Fig. 1 production activated water by Gliding Arc Plasma (GA) and Dielectric Barrier Discharge Plasma (DBD)

Silver nanoparticle synthesis using boiling method

The cyanobacterial cultures in the logarithmic growth phase (14 days) were conducted using activated atmospheric water and distilled water, followed by centrifugation at 2500 rpm for 10 min to collect the biomass. After centrifugation, the residual cyanobacteria were subjected to dehydration in an oven at 60 °C. Subsequently, 1 g of dry weight was heated in 10 ml of double-distilled water for 15 min at 100 °C. Following the boiling process, the mixture was cooled, filtered with filter paper, and subsequently stored in a refrigerator at 4 °C. The extracts devoid of cyanobacteria were subsequently employed in the synthesis of silver nanoparticles. Two milliliters of cyanobacteria-free extract were added to 10 ml of 1 mM silver nitrate solution in 100 ml flasks. The mixture was maintained at 100 °C with continuous agitation. Initially colorless, the solution transitioned to a yellowish-brown hue and ultimately became dark brown after 60 min of shaking. The color change from colorless to brown indicated the formation of silver nanoparticles. The observed color change was recorded, and nanoparticle formation was quantified through spectrophotometry. Silver nanoparticles were harvested via centrifugation at 15,000 rpm for 20 min at 4 °C. The sediment was repeatedly rinsed with distilled water to yield pure silver nanoparticle powder. Spectrophotometry was conducted in the wavelength range of 300 to 800 nm utilizing optical spectroscopy, with distilled water serving as the blank (Fig. 2) [43].

Characterization of AgNPs

The method exhibiting the highest absorption in nanoparticle synthesis, which also demonstrated greater stability over time, was chosen for characterization.

Fourier transform infrared spectroscopy (FTIR)

The functional groups and composition of AgNPs were analyzed using FTIR spectroscopy (Shimadzu, Japan). The AgNPs powders were mixed in potassium bromide at a ratio of 1:100. The FT-IR instrument was operated in diffuse reflectance mode, specifically DRS-800. The spectra were collected over a range of 400 to 4000 $cm-1$ with a resolution of 4 $cm-1$. The identification of functional groups was accomplished by utilizing reference spectra [44].

Dynamic light scattering (DLS) and zeta potential

The size of silver nanoparticles synthesized by cyanobacterial strains was measured. Samples with specific absorption of silver nanoparticles, which were free of settling and had colloidal stability, were selected. Four glass vials containing 5 milliliters of the prepared supernatant with AgNPs were set up. The glass vials were covered with aluminum foil to prevent light penetration and

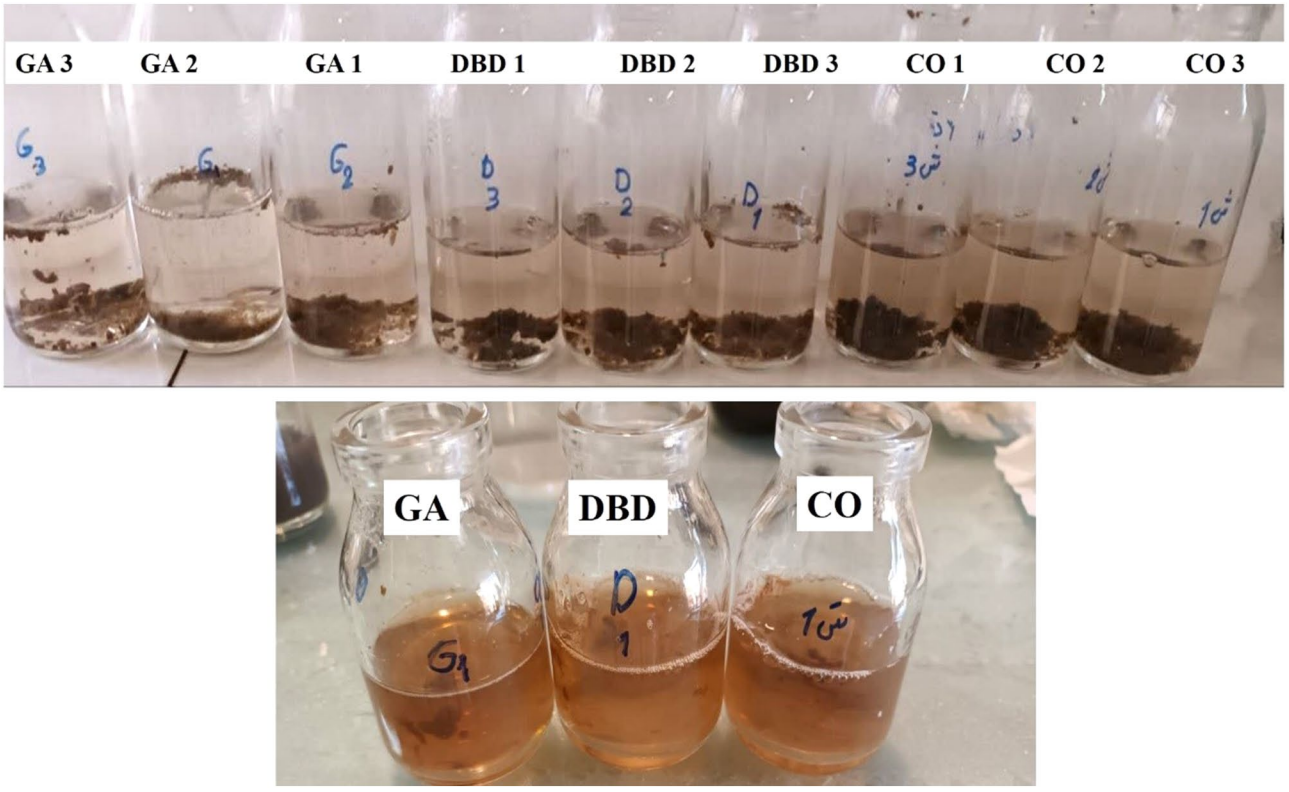

Fig. 2 Synthesizing the nanoparticle from cyanobacteria *Alborzia kermanshahica* using boiling Method. (CO) Control sample, (GA) Sample treated with Gliding Arc Plasma, (DBD) Sample treated with Dielectric Barrier Discharge Plasma. Each treatment underwent three replicated measurements. The color of the solutions turning brown is noticeable in all treatments

particle agglomeration. DLS and zeta potential analysis were performed to assess light scattering and investigate the zeta potential. For this purpose, the Malvern Zetasizer Nano ZS® instrument was used. The measurement parameters included a laser with a wavelength of 633 nm (He–Ne), a constant scattering angle of 135 °, a measurement temperature of 25 °C, a medium viscosity of 0.8872 mPa·s, a medium refractive index of 1.330, and a material refractive index of 1.59. Prior to DLS measurement, the colloid underwent filtration through a 0.2 µm polyvinylidene fluoride (PVDF) membrane. Subsequently, the sample was introduced into a quartz microcuvette [45, 46].

Antibacterial efficiency of AgNPs

The antimicrobial effectiveness of the synthesized AgNPs was assessed using the disk diffusion method against indicator strains of *Staphylococcus aureus*, *Streptococcus mutans* (both Gram-positive bacteria), and *Escherichia coli* and *Klebsiella pneumoniae* (both Gram-negative bacteria). The Kirby-Bauer disk susceptibility test was conducted using standardized procedures. Each petridis was inoculated with 100 µl of a 0.5 McFarland turbidity bacterial suspension (approximately 2×108 cfu/ml) onto nutrient agar plates. The bacterial suspension was evenly spread using a sterile swab. Prepared discs containing AgNPs nanoparticle at a concentration of 20 µg/disc were placed on the inoculated plates at the correct spacing. Then, the plates incubated for 16 h at a temperature of 37 °C. Ultimately, the measurement of the expansion of the inhibition zone around the loaded discs was recorded in mm [47].

Transmission electron microscopy (TEM)

Transmission electron microscopy (TEM, Jeol) was used to capture high-resolution, two-dimensional images of the biosynthesized SNPs. The morphology of the SNPs was visualized using TEM operated at an accelerating voltage of 200 kV. Samples were prepared by adding a drop of SNP suspension onto a carbon-coated copper grid and allowed to dry under an infrared lamp prior to analysis [48].

GC-MS analysis

The chemical composition of the synthesized nanoparticles in the control group and the plasma-treated group were analyzed using a Trace GC1300-TSQ mass spectrometer (Thermo Scientific, Austin, TX, USA) equipped with a direct capillary column (TG-5MS, dimensions: 30 m × 0.25 mm × 0.25 µm film thickness) at 15 (P_{15}) min. The temperature of the column oven was originally

set at 60 °C and then raised at a rate of 5 °C per minute until it reached 200 °C. It was then maintained at this temperature for a duration of 2 min before being further increased to the ultimate temperature of 300 °C at a rate of 20 °C per minute.The final temperature was then maintained for an additional 2 min. The temperatures of the injector and MS transfer line were maintained at 250 °C and 260 °C, respectively. The carrier gas used in this experiment was helium, which was maintained at a consistent flow rate of 1 ml/min. The solvent delay duration was observed to be 3 min, and subsequent to this, diluted samples of 1 µl were automatically injected using an AS1300 autosampler that was paired with a gas chromatograph operating in split mode. Electron ionization (EI) mass spectra were obtained using an ionization voltage of 70 eV. The mass range covered in the analysis was m/z 50–650, and the spectra were acquired in full scan mode. The temperature of the ion source was adjusted to 250 °C. The identification of the components was conducted by comparing their retention durations and mass spectra with those available in the Wiley 09 and NIST 11 mass spectral databases.

Statistical analysis

Results of each representative experiment were analyzed by ANOVA, using the statistical software package SPSS version 24. A confidence interval of 95% was considered to indicate a statistical difference and as a cutoff for rejecting the null hypothesis. The Tukey test was performed to evaluate the significance of difference among mean values when a significant variation ($p<0.05$) was found by the ANOVA test. Each treatment underwent three replicated measurements for which the mean values ± standard error of mean were obtained [49].

Results

Spectroscopy results of synthesized silver nanoparticles from control sample

The results showed that the synthesis of silver nanoparticles using the biomass method and 1 mM silver nitrate did not produce a peak indicating nanoparticle formation at 0 and 12 h in the spectroscopy analysis. At 24, 48, and 72 h, nanoparticle absorption was measured at 430, 433, and 432 nm, with maximum absorbances of 0.728, 0.828, and 0.899, respectively (Figure S1-1). When silver nanoparticles were synthesized with 2 mM silver nitrate for 0 and 12 h, there was no peak in the spectroscopy that indicated nanoparticle synthesis. At 24, 48, and 72 h, nanoparticle absorption was measured at 430, 432, and 433 nm, with maximum absorbances of 0.709, 0.807, and 0.873, respectively (Figure S1-2). Silver nanoparticles synthesized with 3 mM silver nitrate did not show a peak indicating nanoparticle synthesis at 0–12 h. Observations at 24, 48, and 72 h revealed nanoparticle absorption at 432, 430, and 431 nm, with maximum absorbance values of 0.795, 0.788, and 0.905, respectively (Figure S1-3). Figure 3 depicts the spectroscopy of silver nanoparticles

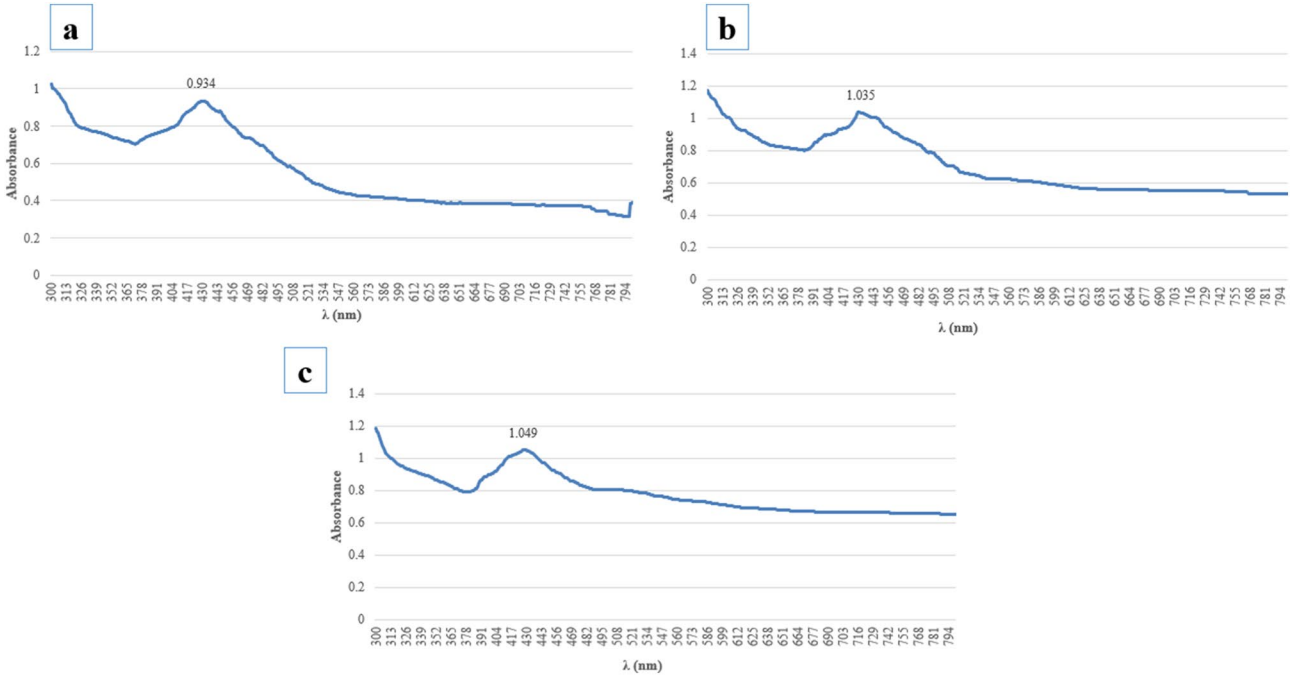

Fig. 3 The spectroscopy results of silver nanoparticles synthesize using the boiling method. (**a**) Control; (**b**) Dielectric Barrier Discharge Plasma; (**c**) gliding arc plasma sample

synthesized through boiling, with nanoparticle absorption at 432 nm and a maximum absorbance of 0.934.

The spectroscopy results for silver nanoparticles synthesized using the dielectric barrier discharge (DBD) plasma method are presented

Figure S2 depicted the spectroscopy results for silver nanoparticles synthesized from an extract of the cyanobacterium *Alborzia kermanshahica* under DBD plasma conditions for 72 h. The wet biomass method was used to synthesize silver nanoparticles under DBD plasma conditions with 1 mM silver nitrate, and the spectroscopy results revealed that no peak indicating nanoparticle synthesis was visible at 0 h. At 12, 24, 48, and 72 h, nanoparticles were absorbed at wavelengths 430, 427, 427, and 429 nm, with maximum absorption values of 0.560, 0.765, 0.857, and 0.899, respectively. Figure S2-1 depicted the spectroscopy results of silver nanoparticles synthesized using the wet biomass method under DBD plasma conditions and 2 mM silver nitrate. At 0 h, no peak was seen. However, at 12, 24, 48, and 72 h, nanoparticle absorption at wavelengths 382, 321, 432, and 435 nm was observed, with maximum absorbance values of 0.560, 0.786, 0.885, and 0.932. Figure S2-2 showed the spectroscopy results for silver nanoparticles synthesized using the wet biomass method under DBD plasma conditions containing 3 mM silver nitrate. Again, no peak was seen at 0 h. However, at 12, 24, 48, and 72 h, nanoparticle absorption at wavelengths 429, 432, 430, and 434 nm was observed, with maximum absorbance values of 0.578, 0.876, 0.920, and 0.975. Figure 3 showed the spectroscopy results for silver nanoparticles synthesized using the boiling method under DBD plasma conditions, with an absorption peak at 432 nm and a maximum absorbance value of 1.035.

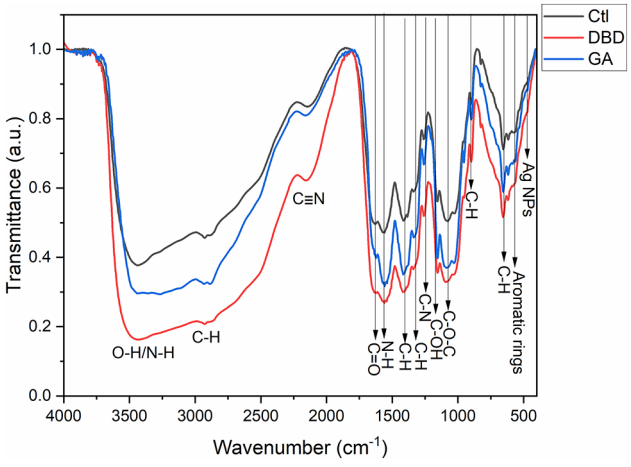

Fig. 4 The FTIR spectroscopy results for silver nanoparticles synthesized using the cyanobacterium *Alborzia kermanshahica*. The black line represents the control sample the blue line shows the sample treated with gliding arc plasma and the red line shows the sample treated with dielectric barrier discharge plasma

Results of spectroscopy for silver nanoparticles synthesized from gliding Arc plasma

The results shown in Figure S3 depicted the spectroscopic analysis of silver nanoparticles produced from the extract of *Alborzia kermanshahica* cyanobacteria using gliding arc plasma conditions over a period of 72 h. Spectroscopic analysis of silver nanoparticles generated through the wet biomass method under gliding arc plasma conditions with 1 mM silver nitrate revealed the absence of nanoparticle synthesis peak at 0 h. Next analysis at 12, 24, 48 and 72 h showed absorption peaks at 433, 427, 427 and 429 nm with corresponding maximum absorption values of 0.678, 0.786, 0.876 and 0.979 respectively.

FTIR results

The spectra of the plasma-treated and control samples showed that no additional peaks appeared following the plasma treatment. This indicated that there were no new functional groups formed on the nanoparticles' surface (as outlined in Table S1). Nevertheless, the intensity of the pre-existing functional group peaks rose, indicating that the plasma treatment reinforced the current bonds on the nanoparticles' surface. These alterations demonstrated that the plasma treatment improved the surface connections without generating new functional groups. According to Fig. 4, the lowest peak intensity for the different bonds was in the control sample, while plasma treatment, whether using dielectric barrier discharge or gliding arc, increased the bond intensity.

Particle size distribution (DLS) results

The particle size distribution results for the silver nanoparticles synthesized by boiling the extract of *Alborzia kermanshahica* under different treatments are shown in Fig. 5 (A). Based on the results, the distribution had a single peak with an average particle size of 196.97 nm and a PDI (polydispersity index) of 0.262, 149.89 nm and a PDI of 0.251, and 226.15 nm and a PDI of 0.296 for control, dielectric barrier discharge plasma, and gliding arc plasma condition, respectively of control, dielectric barrier discharge plasma, and gliding arc plasma condition.

Zeta potential results

The zeta potential results of silver nanoparticles synthesized by boiling the extract from the cyanobacteria *Alborzia kermanshahica* under different treatments are shown in Fig. 5 (B). Based on the results, the zeta potential of the nanoparticles synthesized under control conditions, dielectric barrier discharge plasma, and gliding arc plasma condition were 24.9 mV, 27.7 mV, and 22.5 mV with the electrophoretic mobility of the particles of 0.000195 cm^2/Vs, 0.000201 cm^2/Vs, and 0.000177 cm^2/Vs, respectively.

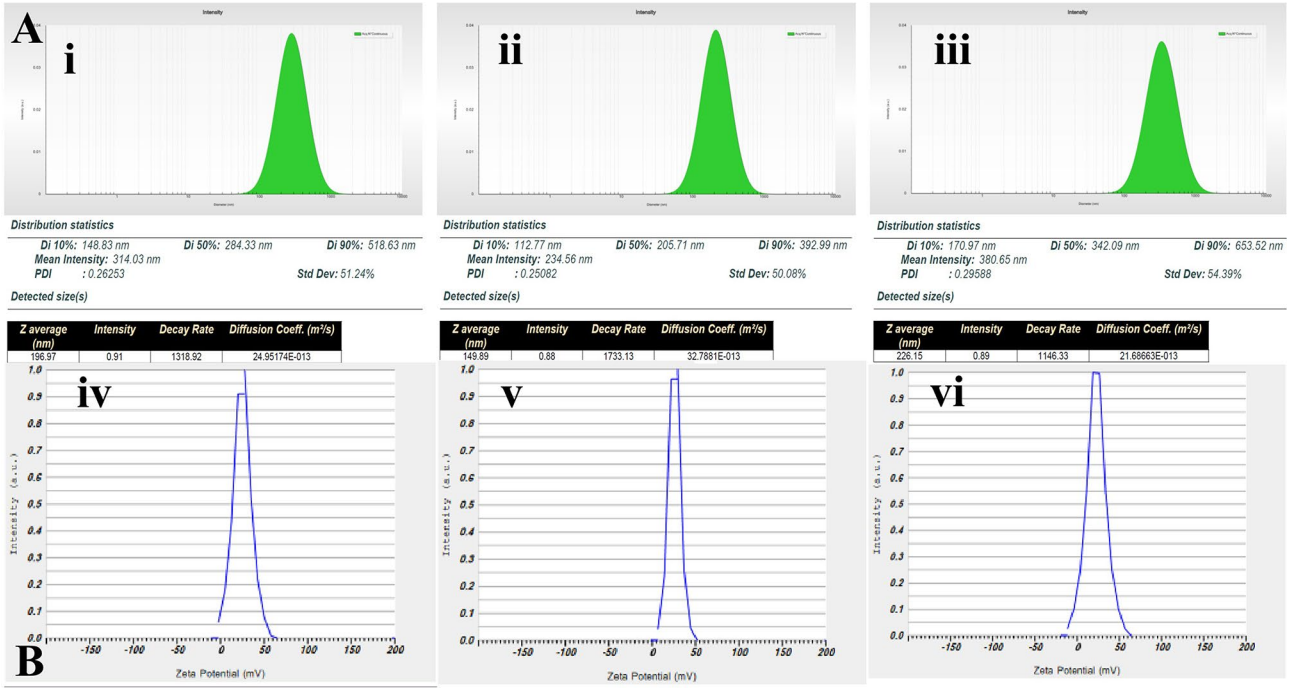

Fig. 5 Results of (**A**) Particle Size Distribution and (**B**) Zeta Potential of Silver Nanoparticles Produced by Boiling from the Cyanobacteria *Alborzia kermanshahica* (i and iv): Control sample, (ii and v): Under Dielectric Barrier Discharge (DBD) Plasma, (iii and vi): Under Gliding Arc Plasma

Table 1 Results of the inhibition zone diameter of the cyanobacterium extract *Alborzia Kermanshahica* under different plasma treatments ($p<0.05$)

Treatment	Diameter of the Inhibition Zone (mm)			
	Klebsiella pneumonia	Escherichia coli	Streptococcus mutans	Staphylococcus aureus
T_1	11.66 ± 0.47^{b}	11.66 ± 0.47^{ab}	11.33 ± 0.47^{b}	12.66 ± 0.47^{ab}
T_2	12.66 ± 0.47^{ab}	12.66 ± 1.00^{a}	13.00 ± 1.00^{ab}	13.66 ± 0.47^{ab}
T_3	12.00 ± 0.00^{b}	12.00 ± 0.47^{ab}	11.66 ± 0.47^{b}	11.33 ± 0.47^{b}
T_4	13.00 ± 0.00^{ab}	12.66 ± 1.00^{a}	13.00 ± 1.00^{ab}	13.66 ± 0.47^{ab}
T_5	12.33 ± 0.47^{ab}	14.33 ± 0.47^{c}	11.66 ± 0.47^{b}	11.66 ± 0.47^{ab}
T_6	13.33 ± 0.00^{a}	13.33 ± 0.47^{a}	12.66 ± 0.47^{a}	12.66 ± 0.47^{ab}

T1: Silver nanoparticles synthesized using the biomass method with 3 mM silver nitrate (control sample); T2: Silver nanoparticles synthesized by boiling (control sample); T3: Silver nanoparticles synthesized using the biomass method with 3 mM silver nitrate under DBD plasma; T4: Silver nanoparticles synthesized by boiling under DBD plasma; T5: Silver nanoparticles synthesized using the biomass method with 3 mM silver nitrate under GA plasma; T6: Silver nanoparticles synthesized by boiling under GA plasma

Different lowercase letters indicate statistical differences in the column ($p<0.05$)

Antibacterial activity results

The results for the diameter of the inhibition zone caused by the extract of the cyanobacterium *Alborzia kermanshahica* under different plasma trwatments on the bacteria *S. aureus*, *S. mutans*, *E. coli* and *K. pneumoniae* are shown in Table 1; Fig. 6. The statistical tests that compared the averages of the different treatments for *Klebsiella pneumonia* showed that the T1 and T6 treatments were significantly different. The T6 treatment had the largest diameter with a significant difference ($p<0.05$). However, the T5 treatment had the highest growth inhibition diameter against *Escherichia coli*, with a significant difference. Moreover, there was no statistically significant difference between different treatments against *Streptococcus mutans* and *Staphylococcus aureus* ($p<0.05$).

TEM test results

The results revealed that the boiling method produced silver nanoparticles with the smallest nanoparticle size and the highest zeta potential in the presence of DBD plasma. Among the pathogens studied, the bacteria *Escherichia coli* had the highest resistance. The study focused on how the silver nanoparticles synthesized by the boiling method under the influence of DBD plasma killed the *Escherichia coli* bacteria. The technique confirmed that the synthesized nanoparticles were spherical. The results showed that the nanoparticles were single, with sizes

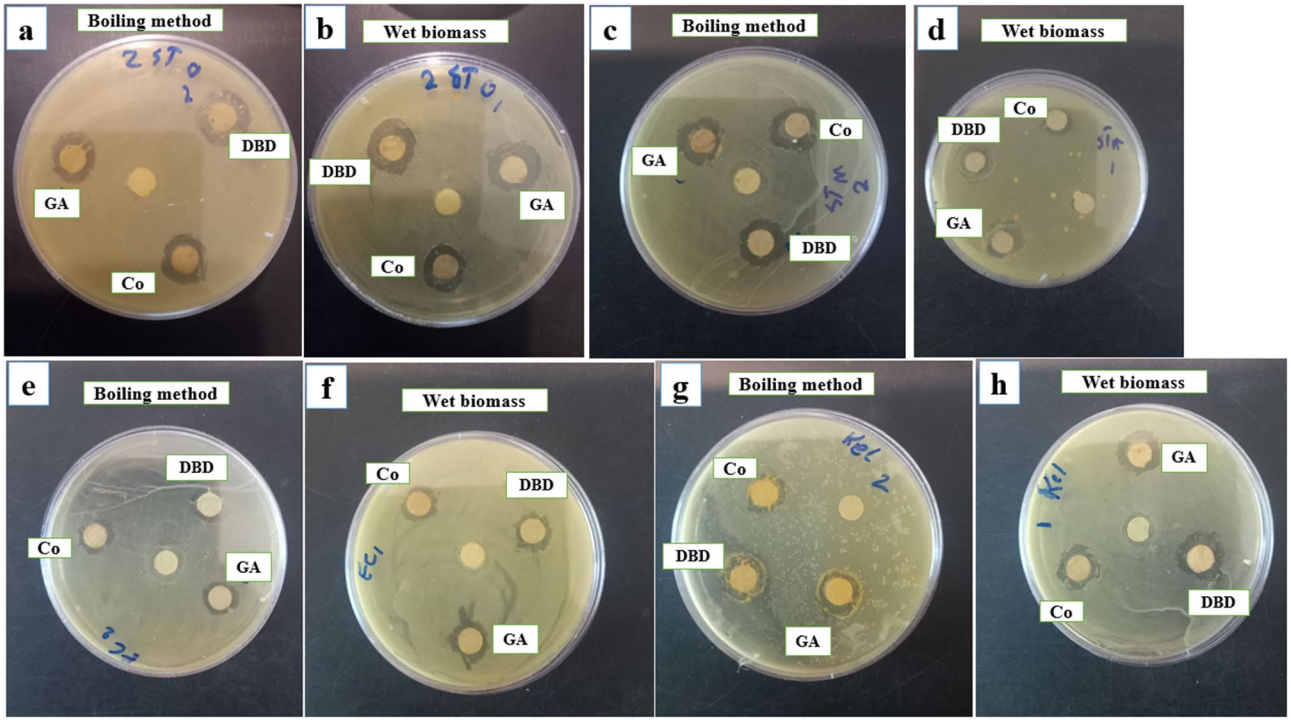

Fig. 6 Diameter of the inhibition zone of silver nanoparticles prepared using wet biomass and boiling methods, on the following bacteria: (**a**-**b**) *Staphylococcus aureus*, (**c**-**d**) *Streptococcus mutans*, (**e**-**f**) *Escherichia coli* and (**g**-**h**) *Klebsiella pneumoniae* under the influence of DBD plasma and GA

ranging from 9.5 to 82 nm, and the average size of the nanoparticles was 30.4 nm (Fig. 7).

GC-MS results

The results of identifying the compounds in the cyanobacteria extract, prepared by boiling under controlled growth conditions, are shown in Figure S4(a) and Table S2. Based on the results, the extraction contained 18 compounds. The most abundant compounds were 2-Methyl-l-propanol, followed by 3-Methylbutanal and 2-Methylbutanal, with frequencies of 14.509% and 13.63%, respectively. The least abundant compound was 2-phenylethanol. The identified compounds under dielectric barrier discharge (DBD) plasma showed that the most abundant were 3-Methylbutanal, followed by 2-Methylbutanal and 2-Methyl-l-propanol with frequencies of 15.052% and 10.491%, respectively. However, The least abundant compound was 1-butanol (Figure S4(b) and Table S3). In addition, The results of identifying the compounds in the cyanobacteria extract prepared by boiling under gliding arc plasma showed that similar to other treatments, 18 compounds were also identified. The most abundant were 3-methylbutanal, followed by 2-methylbutanal and 3-methyl-1-butanol with frequencies of 12.1344% and 11.452%, respectively. The least abundant compound was 2-phenylethanol (Figure S4(c) and Table S4).

Based on the data presented in Table 2, the plasma treatment affected the metabolites of cyanobacteria *Alborzia kermanshahica*. Among the 18 compounds identified in the plasma-treated sample, 6 showed a significant increase and 6 showed a significant decrease in concentration compared to the control. The compounds showing a notable increase are ethyl acetate, 3-methyl-1-butanol, acetic acid, 2-phenylethanol, 1-octen-3-ol, and 3-octen-2-ol. On the other hand, the compounds displaying a significant decrease are methyl acetate, 2-pentanone, ethanol, 1-butanol, 1,3-dimethyl benzene, and 2-methyl-1-propanol. These changes reflect the diverse impacts of plasma on cyanobacteria's metabolism.

Discussion

Silver nanoparticles have garnered significant interest owing to their distinctive physicochemical and biological characteristics. Numerous physicochemical methods have been employed to synthesize nanoparticles of varying shapes and sizes; however, the generation of toxic byproducts has constrained their application. Advancements in nanoparticle synthesis and their growing application across various domains have prompted researchers to assess strategies for enhancing the biocompatibility of these particles. The rise in the utilization of metal nanoparticles has spurred interest in developing environmentally friendly methods for their production. Biological synthesis offers multiple benefits, such as

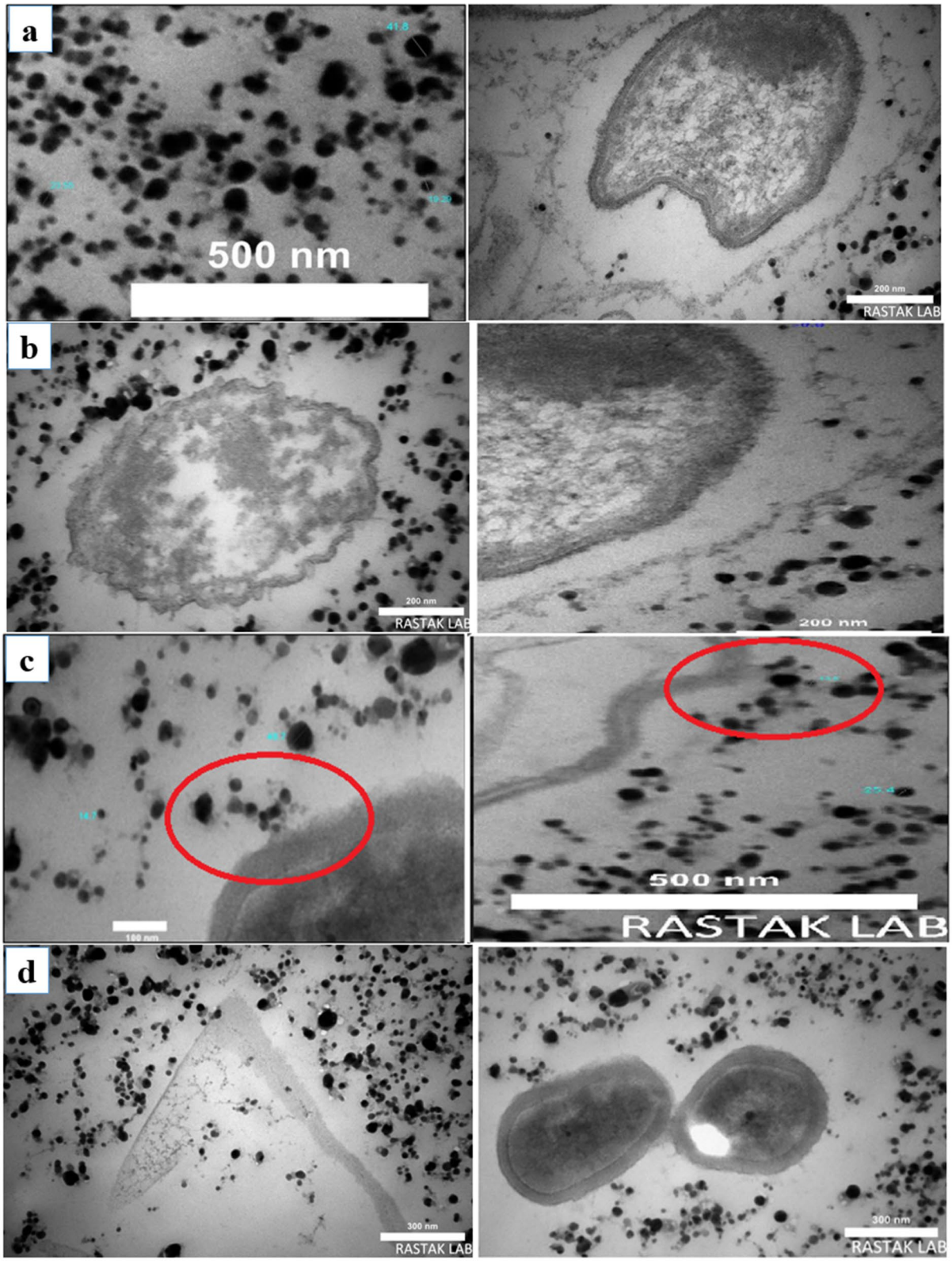

Fig. 7 The results of TEM analysis of silver nanoparticles synthesized by boiling method under DBD plasma. (**a**) synthesized nanoparticles, (**b**) around the membrane of *E.coli* bacteria, (**c**) reaching the membrane of the bacteria and damaging impact on it, (**d**) cell lysis of bacterial cells

Table 2 Changes in compounds identified from *Alborzia kermanshahica* cyanobacteria under plasma treatment compared to the control sample

No	Peak IDs	RT (min)	Control sample	DBD plasma	Plasma GA	Plasma DBD	Change GA
1	2-Methylfuran	4.57	4.496	5.979	4.457	High	Low
2	3-Methylbutanal, 2-methylbutanal	5.14	13.673	15.052	12.134	High	Low
3	Acetic acid methyl ester	7.02	9.698	7.686	8.173	Low	Low
4	Acetic acid ethyl ester	7.41	3.191	3.314	4.377	High	High
5	2-Butanone	8.33	4.520	4.407	5.522	Low	High
6	2-Pentanone	8.87	7.419	7.304	7.175	Low	Low
7	Ethanol	9.24	3.112	2.380	2.996	Low	Low
8	Acetic acid, 3-methylbutyl ester	13.33	2.279	2.141	4.775	Low	High
9	1-butanol	13.82	3.251	2.031	2.356	Low	Low
10	1,3-di methyl benzene	14.68	6.128	3.257	4.500	Low	Low
11	2-Methyl-l-propanol	15.07	14.509	8.597	11.396	Low	Low
12	3-Methyl-1-butanol	15.61	7.705	10.491	11.452	High	High
13	3-Hydroxy-2-butanone	17. 26	3.541	4.818	3.188	High	Low
14	Acetic acid	20.83	2.087	2.759	2.877	High	High
15	Benzaldehyde	22.85	6.271	6.460	3.600	High	Low
16	2-Phenylethanol	28.41	2.007	2.821	2.065	High	High
17	1-Octen-3-ol	28.77	2.526	3.864	4.086	High	High
18	3-Octen-2-ol	29.53	3.589	6.637	4.133	High	High

decreased generation of toxic byproducts, enhanced stability, and lower toxicity to healthy cells [50].

Biologically synthesized silver nanoparticles exhibit notable antimicrobial properties. The antimicrobial properties of silver are inherently present and are further amplified when silver is converted into nanoparticles [17].

Cyanobacteria are being increasingly researched for their high growth rate and biomass productivity, making them an ideal biological model for nanoparticle synthesis. Extracellular synthesis occurs outside the cell, with biological molecules like pigments, ions, proteins, enzymes, hormones, and antioxidants playing a crucial role in reducing nanoparticles. Methods for extracellular synthesis include cell-free culture media, cell biomass extracts, and biomolecules [51]. Therefore, this study was conducted with the aim of applying cold atmospheric plasma technology on the antimicrobial activity of silver nanoparticles biosynthesized by the cyanobacterium *Alborzia kermanshahica.*

Localized Surface Plasmon Resonance Spectroscopy (LSPR) is a method for detecting chemical and biological molecules by measuring the surface plasmon resonance of metal nanoparticles. Surface plasmons are confined to the surface and strongly interact with light rays coming to the metal surface. Light with a frequency lower than the surface plasmon frequency is reflected by the metal, as electrons on the metal surface block the light electric field. LSPR is produced on metal nanostructures after light irradiation, causing collective electron charge fluctuations. The results indicated that boiling and treatment with gliding arc plasma yielded the most favorable outcomes for spectroscopy. The observed UV peak at 435 nm following the synthesis of silver nanoparticles may result from the interaction of the extracts employed in their coating. Exopolysaccharides are proposed to contribute to the reduction and stabilization of nanoparticles. These complex polymers may include amino sugar components as well as non-carbohydrate compounds such as phosphate, lactate, acetate, and glycerol [52].

The research indicated that the nanoparticles exhibited a spherical morphology. Increased extraction time and concentration resulted in larger nanoparticles, consistent with the findings from nanoparticle morphology observed via TEM. In comparison to our results, Sahoo and colleagues (2020) reported that the synthesized silver nanoparticles from the extract of *Cyanobacterium pikei* had a peak at 420 nm. They reported that over 48 to 56 h, active compounds in the cyanobacterium reduced Ag ions to Ag(0) [41]. Also, Singh and colleagues (2020) found that the biosynthetic silver nanoparticles using *Leptolyngbya sp*. showed a peak at 430 nm in the absorption spectrum due to the plasmonic enhancement of the nanoparticles, possibly because of the presence of mycosporine-like amino acids (MAAs) in the cell extract [53].

The FT-IR analysis was used to study the chemical bonds in the synthesized nanoparticles. The broad peak at wave number 3440 corresponds to the stretching vibration of O-H and N-H bonds in cyanine, alcoholic, and acidic structures in organic compounds used for green synthesis. Other peaks at 2930 cm-1 and 2860 cm-1 relate to the asymmetric and symmetric stretching vibrations of C-H bonds in methyl and methylene structures. The peak at 2160 cm-1 is a characteristic

peak of a triple bond, while the peak at 1580 cm-1 is related to the bending vibration of N-H bonds in amine structures. The peaks at 1155 cm-1 and 1093 cm-1 correspond to the stretching vibrations of C-OH and C-O-C bonds. The main compounds in the samples are C-OH, C=O, C-H, O-H, C-O-C, and aromatic rings.Therefore, from the results of the FTIR test, the presence of organic compounds on the surface of nanoparticles as a capping agent can be proven.

The spectra of the plasma-treated and control samples clearly show that the plasma treatment did not produce any new peaks, indicating the formation of no new functional groups on the nanoparticles. Figure 4 shows that the lowest intensity of peaks related to different bonds was in the control sample (not treated with plasma). Plasma treatments, whether DBD or GA, increased the bond intensities. Generally, the more bonds there are in the structure, the higher the intensity in the FTIR spectrum. This means that plasma treatment increased the number of organic bonds on the silver nanoparticles that were made by green synthesis. This made the particles more evenly dispersed and made the silver particles in suspension smaller and more stable [54]. This was confirmed by other tests. Moreover, DBD-treated samples had higher peak intensities compared to GA-treated samples, suggesting that DBD is better than GA for increasing functional groups on silver nanoparticles. In comparison to our study, the FTIR results of synthesis silver nanoparticles from Cyanobacteria *Desertifilum* sp. extract by Reham Samir Hamida et al. (2020) showed that polysaccharides and proteins may have contributed to the biofabrication of nanoparticles [48]. Also, Debasish Borah et al.'s (2023) FTIR analysis for silver nanoparticles produced from *Nostoc carneum* indicated the presence of phytochemicals on the AgNPs surface, which served as both reducing and capping agents [55].

DLS analysis is a physical method used to determine the distribution of particles in solutions and suspensions. It involves evaluating the scattering and intensity changes of laser light based on the Brownian motion of particles, which is then used to calculate the particle dimensions. The Brownian motion of particles depends on the size of the particles, with larger particles causing slower motion and smaller particles causing faster movement. Other factors like temperature and viscosity also affect the Brownian motion. The size of a particle is related to dispersion time, with smaller molecules dispersing faster than larger ones. The concentration of bioregenerative substances also affects the size of synthesized particles, with smaller particles having more antibacterial activity [56]. With respect to particle size distribution characterization, a parameter used to define the size range of the lipidic nanocarrier systems is called the "polydispersity index" (PDI). The term "polydispersity" (or "dispersity" as recommended by IUPAC) is used to describe the degree of non-uniformity of a size distribution of particles. The PDI value may vary from 0 to 1, where colloidal particles with a PDI less than 0.1 indicate monodisperse particles and values greater than 0.1 may indicate a polydisperse particle size distribution [57]. Studies have shown that when the PDI value is less than 0.3, it indicates that the degree of dispersion is good [58]. DLS can be inaccurate for uniform nanoparticles due to its inability to distinguish between nanoparticles with slight differences in diameter and not accurately representing multipart samples. This is because the intensity of scattered light is proportional to six times the diameter of the particle, which can superimpose light from larger particles or agglomeratization. DLS measures the hydrodynamic diameter of particles containing hydration layers, polymer shells, or other stabilizers, leading to larger nanoparticles. This results in larger DLS sizes than SEM and TEM, as it measures all biological molecules in the liquid sample. Therefore, DLS sizes are often larger than those from SEM and TEM [59]. Aly and colleagues (2023) reported that the synthesis of silver nanoparticles using *Nostoc muscorum* had a diameter of 60 nm. They noted that DLS sizes are usually larger than those from SEM and TEM due to the solvent layer attached to the particles [60]. Husain and colleagues (2021) showed that $AgNO_3$ concentration plays an important role in synthesizing and reducing the size of nanoparticles [61]. Ameen and colleagues (2020) reported that the average particle size of silver nanoparticles synthesized with *Spirulina platensis* was 74.8 nm with a PDI of 0.285 [62]. The size difference between TEM and DLS measurements may be due to DLS analyzing scattered light in water while TEM is a local analysis of the particles.

Zeta potential is a measure of the electric charge on a nanoparticle surface, which quantifies the charges. It is determined by the concentration of oppositely charged ions near the nanoparticle surface. The zeta potential is the difference between the bulk fluid and the fluid layer containing oppositely charged ions. The liquid layer around a particle consists of an inner (Stern layer) and outer (diffuse) region. In the scattered layer, a hypothetical boundary forms between ions and particles. When a particle moves due to gravity, the ions within the boundary move it, leaving the ions beyond the boundary with the mass spreader. The zeta potential indicates the potential stability of the colloidal system. Particles with a positive zeta potential repel each other, while those with a negative zeta potential prevent agglomeration and coagulation. The dividing line between stable and unstable suspensions is usually+30 or -30 mV [63].

The zeta potential results showed that all obtained nanoparticles had positive zeta potentials, indicating a positive charge of the particles in suspension. Ismail and

colleagues (2021) found zeta potentials of -15.902 mV and −16.811 mV for S. *platensis* and N. *linkia*, which is similar to our study and showed that they were stable [64]. El-Sheekh and colleagues (2021) reported a zeta potential of 29 mV for silver oxide nanoparticles synthesized from *Oscillatoria* sp [65]. Also, Ameen and colleagues (2020) showed that silver nanoparticles produced using the cyanobacterium *Spirulina platensis* had a zeta potential of -46.04 mV. This means that the produced nanoparticles were very stable. The negative zeta potential might be due to the type of reducing agents in the extract, such as proteins. Furthermore, the nanoparticles' negative zeta potential may be due to the extract's functional groups, which cause deprotonation [62].

TEM (Transmission Electron Microscopy) is a high-resolution imaging technique used to measure nanoparticle size, grain size, size distribution, and morphology. It confirms the sphericity and aggregation of synthesized nanoparticles from cyanobacteria extract, as reported in various studies [42]. The results of TEM images confirmed that the silver nanoparticles were spherical and clustered together. Other studies have also reported this clustering of nanoparticles made from cyanobacteria extracts (Patel et al., 2015). The size of the nanoparticles, as shown by TEM, ranged from 9.5 to 82 nm.

The exact mechanisms of CP mediated bacterial inactivation are still under investigation, but several generated products have been demonstrated to play a role. These products include ROS, RNS, UV radiation and charged particles within a plasma gas phase. Among the ROS, ozone, atomic oxygen, singlet oxygen, superoxide, peroxide, and hydroxyl radicals, are considered to be involved in bacterial inactivation [28, 66]. Shweta B. Borkar et al. (2024) investigated the properties of DBD plasma-generated nitric oxide water treatment on the survival and virulence of *S. enterica*, *S. flexneri*, and *V. parahaemolyticus* bacteria. They showed that RNS generated from PG-NOW might be beneficial for preventing diarrheal infections [67]. Charged particles, electrons, and ions can disrupt the cell wall of bacteria, breaking chemical bonds and causing erosion through etching. This can lead to the formation of lesions and openings in the membranes, allowing the penetration of plasma toxic compounds. Gram-negative bacteria are more susceptible to erosion due to their vulnerability, while Gram-positive bacteria are more affected by higher intracellular ROS levels [68]. Charged particles can also cause mechanical disruption of bacterial cell membranes, with indirect treatment designs using distance or metal mesh to avoid direct contact. Etching, a reaction between excited atoms and radicals, can break bonds, leading to morphological changes such as cell size reduction, deep channels, and cellular destruction [69]. Atomic oxygen and ozone react with open bonds, facilitating faster etching of molecules. This erosion effect can also lead to the demise of microbial support structures like biofilms [20]. Despite the extensive research on the antimicrobial effects of CP [70, 71], it is necessary to consider this technology in tandem with the nature of the microbial cvontamination presented in foods, their processing environments as well as clinical and healthcare situations to elucidate how the mechanisms and mode of delivery may be optimized to provide effective alternative antimicrobial technologies [28, 72].

There exist few mechanisms of antibacterial activity of nanoparticles. They may result in bacterial cell wall or membrane damage or be responsible for detrimental changes in cellular.

organelles. However, it should be noted that some of these mechanisms are speculative and need further thorough examination. The mechanisms of nanoparticles antibacterial activity are frequently discussed in the literature on the example of metallic Ag nanoparticles [73]. One of the cytotoxic mechanism is the result of Ag nanoparticles uptake by the bacterial cells as they are able to penetrate the bacterial cell wall. The degree of dispersion of NPs in water solution seems to play an important role in antibacterial mechanism. However the scientists' opinions are ambiguous. Lee et al. (2010) indicated that the antibacterial efficacy of silver nanoparticles depend on the aggregation degree between nanoparticles; in well dispersed nanoparticles solution more efficient transport to the bacteria cell wall is provided compared to the nanoparticles agglomerates [74]. On the contrary, Marius et al. (2011) in his work describing enhanced antibacterial effect of silver nanoparticles claimed that the major mechanism responsible for this effect probably consists in clusters formation and nanoparticles anchorage to the bacterial cell surface [75].

The effectiveness of silver nanoparticles against pathogenic microorganisms (such as *Staphylococcus aureus*, *Streptococcus mutans*, *Klebsiella pneumoniae* and *Escherichia coli*) was examined in this research. Significant statistical differences were reported between different treatments. All pathogens were more sensitive to treatments using plasma and boiling methods and showed less resistance. Among the pathogens studied, the bacteria *Escherichia coli* had the highest resistance, so the E. *coli* was chosen as a model to study the effect of silver nanoparticles on the permeability and membrane structure of E. coli cells by TEM analysis (Fig. 7). Recent studies have shown that the antibacterial effect of silver nanoparticles depends more on their size, with smaller particles being more effective. Silver nanoparticles smaller than 10 nm have a direct interaction with bacteria, leading to electronic effects that enhance their reactivity [76]. The enhanced antimicrobial activity of silver nanoparticles is attributed to these electronic effects when they are prepared by boiling [77]. In comparison

to our study, El-Naggar and colleagues (2017) reported that the presence of phycobiliproteins in cyanobacterial extracts might help anchor coated nanoparticles onto bacterial cell membranes enhancing their antibacterial activity [78]. Hamida and colleagues (2020) also found that silver nanoparticles made from the cyanobacterium *Desertifilum sp* had antibacterial properties against five bacteria (*Bacillus cereus*, *Pseudomonas aeruginosa*, *Shigella flexneri*, *Salmonella enterica* and *Bacillus subtilis*) [48]. Aletayeb and colleagues (2020) found that silver nanoparticles (AgCl/AgPO4) made by two different strains of the cyanobacterium *Nostoc* sp. were tested for their ability to kill bacteria. The nanoparticles made by the *Nostoc pruniforme* strain were better at stopping bacterial growth compared to those made by the *Nostoc* M5094-IBRC strain. The researchers concluded that Ag_3PO4 nanoparticles are very important for their antibacterial properties. They also showed that the concentration needed to kill bacteria (MBC) was the same as the concentration needed to inhibit bacterial growth (MIC) [79]. Karageorgou and colleagues (2022) showed that silver nanoparticles made from the cyanobacterium *Pseudanabaena*/*Limnothrix* sp. had antibacterial effects at low concentrations and for short periods against both gram-positive and gram-negative bacteria [80].

The results of the analysis of the compounds in the tested samples of control, DBD plasma and GA plasma revealed 18 compounds of 2-methylfuran, 3-methylbutanal, 2-methylbutanal, acetic acid methyl ester, acetic acid ethyl ester, 2-butanone, 2-pentanone, ethanol, acid Acetic acid, 3-methylbutyl ester, 1-butanol, 3,1-dimethylbenzene, 2-methyl-l-propanol, 3-methyl-1-butanol, 3-hydroxy-2-butanone, acetic acid, benzaldehyde, 2-Phenylethanol, 1-octene-ol, 3-octene-2-ol, 4-octene-3-one. Based on the results, there was no qualitative difference between the compounds in the plasma-activated samples and the control but the quantities of the samples varied [80].

Conclusion

Cyanobacteria, or blue-green algae, are known for their ability to produce nanoparticles due to their biomass productivity and bioremediation of hazardous metals. Silver nanoparticles (Ag-NPs) are highly regarded for their antimicrobial and anticancer properties in the medical sector. These nanoparticles exhibit efficient antibacterial activity through various mechanisms, such as forming free radicals, increasing cell membrane permeability, and disrupting cell proteins through binding with thiol and amino groups. Cold plasmas technology and cyanobacterial sp. silver nanoparticles could offer a potential method for microbial decontamination by generating reactive oxygen and nitrogen species. Therefore, the goal of this research was to utilize atmospheric cold plasma technology to boost the antibacterial effectiveness of silver nanoparticles produced by the cyanobacterium *Alborzia kermanshahica*. The results showed that both types of plasma (DBD and GA) improved the antibacterial properties of the silver nanoparticles. DBD plasma significantly improved the antibacterial activity, producing smaller and more stable nanoparticles that were more effective against gram-positive and gram-negative bacteria. Nanoparticles made using GA plasma, while having the highest spectral peak, had larger sizes and less antibacterial activity. The study suggested that combining nanoparticle synthesis with atmospheric cold plasma technology can enhance the antibacterial properties of Iranian cyanobacterium strains against pathogenic bacteria, providing a potential alternative to chemical antibiotics.

Supplementary Information

The online version contains supplementary material available at https://doi.org/10.1186/s12896-024-00905-x.

Supplementary Material 1

Acknowledgements
Not applicable.

Author contributions
B. N. Conceptualization, methodology, software, formal analysis, investigation, writing—original draft preparation, H.B, F.M.A, R.B. do some investigation. All Authors confirm that all methods were carried out in accordance with relevant guidelines and regulations.

Funding
Not applicable.

Data availability
All data generated or analysed during this study are included in this published article.

Declarations

Ethics approval and consent to participate
All methods were carried out in accordance with relevant guidelines and regulations. Authors don't do any experiments on humans and/or the use of human tissue samples.

Consent for publication
Not applicable.

Competing interests
The authors declare no competing interests.

Live vertebrates and/or higher invertebrates
This study is not on live vertebrates and/or higher invertebrates.

Images
All the images are original and not copy from other papers.

Author details
[1]Department of Biotechnology, Faculty of Converging Sciences and Technologies, Islamic Azad University, Science and Research Branch, Tehran, Iran

Received: 16 August 2024 / Accepted: 1 October 2024

Published online: 07 October 2024

References

1. Nowruzi B. A review of bioactive compounds of cyanobacteria and microalgae as cosmetically useful supplements. J Dermatology Cosmet. 2022;12(4):256–69.
2. Anvar SAA, Nowruzi B, Afshari G. A review of the application of nanoparticles biosynthesized by microalgae and cyanobacteria in medical and veterinary sciences. 2023.
3. Eydelkhani M, Kiabi S, Nowruzi B. In vitro assessment of the effect of magnetic fields on efficacy of biosynthesized selenium nanoparticles by Alborzia Kermanshahica. BMC Biotechnol. 2024;24(1):27.
4. Bin-Meferij MM, Hamida RS. Biofabrication and antitumor activity of silver nanoparticles utilizing novel nostoc sp. Bahar M. Int J Nanomed 2019:9019–29.
5. Gharpure S, Akash A, Ankamwar B. A review on antimicrobial properties of metal nanoparticles. J Nanosci Nanotechnol. 2020;20(6):3303–39.
6. El-Belely EF, Farag MM, Said HA, Amin AS, Azab E, Gobouri AA, Fouda A. Green synthesis of zinc oxide nanoparticles (ZnO-NPs) using Arthrospira platensis (class: Cyanophyceae) and evaluation of their biomedical activities. Nanomaterials. 2021;11(1):95.
7. Asif N, Ahmad R, Fatima S, Shehzadi S, Siddiqui T, Zaki A, Fatma T. Toxicological assessment of Phormidium sp. derived copper oxide nanoparticles for its biomedical and environmental applications. Sci Rep. 2023;13(1):6246.
8. Borah D, Saikia P, Sarmah P, Gogoi D, Das A, Rout J, Ghosh NN, Pandey P, Bhattacharjee CR. Photocatalytic and antibacterial activity of fluorescent CdS quantum dots synthesized using aqueous extract of cyanobacterium Nostoc carneum. Bionanoscience. 2023;13(2):650–66.
9. Yonathan K, Mann R, Mahbub KR, Gunawan C. The impact of silver nanoparticles on microbial communities and antibiotic resistance determinants in the environment. Environ Pollut. 2022;293:118506.
10. Ahmed MW, Soroor AS. Silver nanoparticles, synthesis, characterization and applications. Bull Fac Sci Zagazig Univ. 2024;2023(4):200–20.
11. Garg D, Sarkar A, Chand P, Bansal P, Gola D, Sharma S, Khantwal S, Surabhi, Mehrotra R, Chauhan N. Synthesis of silver nanoparticles utilizing various biological systems: mechanisms and applications—a review. Prog Biomater. 2020;9:81–95.
12. Mazkad D, Lazar N, Benzaouak A, Touach N, El Mahi M, Lotfi E. Silver Nps assembled lithium niobate Ag@ LiNbO3 photocatalysts for visible light-assisted pharmaceutical degradation. J Photochem Photobiol A. 2024;453:115662.
13. Rivera-Mendoza D, Quiñones B, Huerta-Saquero A, Castro-Longoria E. Antimicrobial activity of Green Synthesized Silver and Copper Oxide nanoparticles against the Foodborne Pathogen Campylobacter jejuni. Antibiotics. 2024;13(7):650.
14. Velusamy P, Kumar GV, Jeyanthi V, Das J, Pachaiappan R. Bio-inspired green nanoparticles: synthesis, mechanism, and antibacterial application. Toxicol Res. 2016;32(2):95–102.
15. Pathak J, Ahmed H, Singh DK, Pandey A, Singh SP, Sinha RP. Recent developments in green synthesis of metal nanoparticles utilizing cyanobacterial cell factories. Nanomaterials Plants Algae Microorganisms 2019:237–65.
16. Hanna AL, Hamouda HM, Goda HA, Sadik MW, Moghanm FS, Ghoneim AM, Alenezi MA, Alnomasy SF, Alam P, Elsayed TR. Biosynthesis and characterization of silver nanoparticles produced by Phormidium ambiguum and Desertifilum tharense cyanobacteria. Bioinorg Chem Appl. 2022;2022(1):9072508.
17. Younis NS, Mohamed ME, El Semary NA. Green synthesis of silver nanoparticles by the cyanobacteria synechocystis sp.: characterization, antimicrobial and diabetic wound-healing actions. Mar Drugs. 2022;20(1):56.
18. Sidorowicz A, Margarita V, Fais G, Pantaleo A, Manca A, Concas A, Rappelli P, Fiori PL, Cao G. Characterization of nanomaterials synthesized from Spirulina platensis extract and their potential antifungal activity. PLoS ONE. 2022;17(9):e0274753.
19. El-Sheekh MM, El-Kassas HY. Algal production of nano-silver and gold: their antimicrobial and cytotoxic activities: a review. J Genetic Eng Biotechnol. 2016;14(2):299–310.
20. Anuntagool J, Srangsomjit N, Thaweewong P, Alvarez G. A review on dielectric barrier discharge nonthermal plasma generation, factors affecting reactive species, and microbial inactivation. Food Control. 2023;153:109913.
21. Aggelopoulos CA. Recent advances of cold plasma technology for water and soil remediation: a critical review. Chem Eng J. 2022;428:131657.
22. Misra N, Schlüter O, Cullen P. Plasma in food and agriculture. Cold plasma in food and agriculture. Elsevier; 2016. pp. 1–16.
23. Bermudez-Aguirre D. Advances in cold plasma applications for food safety. and preservation: Academic; 2019.
24. Brandenburg R. Dielectric barrier discharges: progress on plasma sources and on the understanding of regimes and single filaments. Plasma Sources Sci Technol. 2017;26(5):053001.
25. Šimončicová J, Kryštofová S, Medvecká V, Ďurišová K, Kaliňáková B. Technical applications of plasma treatments: current state and perspectives. Appl Microbiol Biotechnol. 2019;103:5117–29.
26. Subedi DP, Joshi UM, Wong CS. Dielectric barrier discharge (DBD) plasmas and their applications. Plasma Sci Technol Emerg Economies: An AAAPT Experience 2017:693–737.
27. Punia Bangar S, Suri S, Nayi P, Phimolsiripol Y. Cold plasma for microbial safety: Principle, mechanism, and factors responsible. J Food Process Preserv. 2022;46(12):e16850.
28. Bourke P, Ziuzina D, Han L, Cullen P, Gilmore BF. Microbiological interactions with cold plasma. J Appl Microbiol. 2017;123(2):308–24.
29. Das S, Gajula VP, Mohapatra S, Singh G, Kar S. Role of cold atmospheric plasma in microbial inactivation and the factors affecting its efficacy. Health Sci Rev. 2022;4:100037.
30. Acharya TR, Jang M, Lee GJ, Choi EH. A comprehensive study on the synthesis, characteristics, and catalytic applications of submerged hydrogen-mixed argon plasma-synthesized silver nanoparticles. Curr Appl Phys. 2023;56:36–46.
31. Ma C, Nikiforov A, De Geyter N, Morent R, Ostrikov KK. Plasma for biomedical decontamination: from plasma-engineered to plasma-active antimicrobial surfaces. Curr Opin Chem Eng. 2022;36:100764.
32. Elg DT, Delgado HE, Martin DC, Sankaran RM, Rumbach P, Bartels DM, Go DB. Recent advances in understanding the role of solvated electrons at the plasma-liquid interface of solution-based gas discharges. Spectrochimica Acta Part B: at Spectrosc. 2021;186:106307.
33. Jawaid P, Rehman MU, Zhao Q-L, Misawa M, Ishikawa K, Hori M, Shimizu T, Saitoh J-i, Noguchi K, Kondo T. Small size gold nanoparticles enhance apoptosis-induced by cold atmospheric plasma via depletion of intracellular GSH and modification of oxidative stress. Cell Death Discovery. 2020;6(1):83.
34. Simeni MS, Zheng Y, Barnat EV, Bruggeman PJ. Townsend to glow discharge transition for a nanosecond pulse plasma in Helium: space charge formation and resulting electric field dynamics. Plasma Sources Sci Technol. 2021;30(5):055004.
35. Shaker AH, Aadim KA. Synthesis and characterization of aluminum oxide nanoparticles prepared by two different cold plasma jet methods. Iraqi J Phys. 2024;22(1):20–30.
36. Acharya TR, Lamichhane P, Jaiswal A, Kaushik N, Kaushik NK, Choi EH. Evaluation of degradation efficacy and toxicity mitigation for 4-nitrophenol using argon and air-mixed argon plasma jets. Chemosphere. 2024;358:142211.
37. Nowruzi B, Soares F. Alborzia Kermanshahica gen. nov., sp. nov.(Chroococcales, Cyanobacteria), isolated from paddy fields in Iran. Int J Syst Evol MicroBiol. 2021;71(6):004828.
38. Lázár D, Takács E, Mörtl M, Klátyik S, Barócsi A, Kocsányi L, Lenk S, Domján L, Szarvas G, Lengyel E. Application of a fluorescence-based instrument prototype for chlorophyll measurements and its utility in an herbicide algal ecotoxicity assay. Water. 2023;15(10):1866.
39. Seifi G, Nowruzi B, Bagheri F. The effect of dielectric barrier discharge plasma treatment on Dulcicalothrix Alborzica (Nostocales, cyanobacteria) under lead stress. Bioremediat J 2024:1–14.
40. Maroofi A, Navab Safa N, Ghomi H. Atmospheric air plasma jet for improvement of paint adhesion to aluminium surface in industrial applications. Int J Adhes Adhes 2020, 98.
41. Sahoo CR, Maharana S, Mandhata CP, Bishoyi AK, Paidesetty SK, Padhy RN. Biogenic silver nanoparticle synthesis with cyanobacterium Chroococcus minutus isolated from Baliharachandi sea-mouth, Odisha, and in vitro antibacterial activity. Saudi J Biol Sci. 2020;27(6):1580–6.
42. Patel V, Berthold D, Puranik P, Gantar M. Screening of cyanobacteria and microalgae for their ability to synthesize silver nanoparticles with antibacterial activity. Biotechnol Rep. 2015;5:112–9.
43. Geetha S, Vijayakumar K, Aranganayagam K, Thiruneelakandan G. Biosynthesis, characterization of silver nanoparticles and antimicrobial screening by Oscillatoria Annae. In: AIP Conference Proceedings: 2020. AIP Publishing.
44. Al-Dhafri K, Ching CL. Phyto-synthesis of silver nanoparticles and its bioactivity response towards nosocomial bacterial pathogens. Biocatal Agric Biotechnol. 2019;18:101075.

45. Husain S, Verma SK, Yasin D, Rizvi MMA, Fatma T. Facile green bio-fabricated silver nanoparticles from Microchaete infer dose-dependent antioxidant and anti-proliferative activity to mediate cellular apoptosis. Bioorg Chem. 2021;107:104535.
46. Ismail A, Saputri L, Dwiatmoko A, Susanto B, Nasikin M. A facile approach to synthesis of silica nanoparticles from silica sand and their application as superhydrophobic material. J Asian Ceam Soc. 2021;9(2):665–72.
47. Ahmad H, Venugopal K, Rajagopal K, De Britto S, Nandini B, Pushpalatha HG, Konappa N, Udayashankar AC, Geetha N, Jogaiah S. Green synthesis and characterization of zinc oxide nanoparticles using Eucalyptus globules and their fungicidal ability against pathogenic fungi of apple orchards. Biomolecules. 2020;10(3):425.
48. Hamida RS, Abdelmeguid NE, Ali MA, Bin-Meferij MM, Khalil MI. Synthesis of silver nanoparticles using a novel cyanobacteria Desertifilum sp. extract: their antibacterial and cytotoxicity effects. Int J Nanomed 2020:49–63.
49. Nowruzi B, Khavari-Nejad R, Sivonen K, Kazemi B, Najafi F, Nejadsattari T. Optimization of cultivation conditions to maximize extracellular investments of two Nostoc strains. Arch Hydrobiol Suppl Algol Stud. 2013;142(1):63–76.
50. Aarthye P, Sureshkumar M. Green synthesis of nanomaterials: An overview. *Materials Today: Proceedings* 2021, 47:907–913.
51. Beyrer M, Pina-Perez MC, Martinet D, Andlauer W. Cold plasma processing of powdered Spirulina algae for spore inactivation and preservation of bioactive compounds. Food Control. 2020;118:107378.
52. Cepoi L, Rudi L, Chiriac T, Valuta A, Zinicovscaia I, Duca G, Kirkesali E, Frontasyeva M, Culicov O, Pavlov S, et al. Biochemical changes in cyanobacteria during the synthesis of silver nanoparticles. Can J Microbiol. 2015;61(1):13–21.
53. Singh Y, Kaushal S, Sodhi RS. Biogenic synthesis of silver nanoparticles using cyanobacterium Leptolyngbya sp. WUC 59 cell-free extract and their effects on bacterial growth and seed germination. Nanoscale Adv. 2020;2(9):3972–82.
54. Sonawane A, Mujawar MA, Bhansali S. Effects of cold atmospheric plasma treatment on the morphological and optical properties of plasmonic silver nanoparticles. Nanotechnology. 2020;31(36):365706.
55. Borah D, Das N, Sarmah P, Ghosh K, Chandel M, Rout J, Pandey P, Ghosh NN, Bhattacharjee CR. A facile green synthesis route to silver nanoparticles using cyanobacterium Nostoc carneum and its photocatalytic, antibacterial and anticoagulative activity. Mater Today Commun. 2023;34:105110.
56. El Semary NA, Bakir EM. Multidrug-resistant bacterial pathogens and public health: the antimicrobial effect of cyanobacterial-biosynthesized silver nanoparticles. Antibiotics. 2022;11(8):1003.
57. Raval N, Maheshwari R, Kalyane D, Youngren-Ortiz SR, Chougule MB, Tekade RK. Importance of physicochemical characterization of nanoparticles in pharmaceutical product development. Basic fundamentals of drug delivery. Elsevier; 2019. pp. 369–400.
58. Danaei M, Motaghi MM, Naghmachi M, Amirmahani F, Moravej R. Green synthesis of silver nanoparticles (AgNPs) by filamentous algae extract: Comprehensive evaluation of antimicrobial and anti-biofilm effects against nosocomial pathogens. Biologia. 2021;76(10):3057–69.
59. Lazcano-Ramírez HG, Garza-García JJ, Hernández-Díaz JA, León-Morales JM, Macías-Sandoval AS, García-Morales S. Antifungal activity of Selenium nanoparticles obtained by plant-mediated synthesis. Antibiotics. 2023;12(1):115.
60. Aly BE, Mona BH, Higazy AM. Green synthesis of silver nanoparticles by cyanobacterial extracts: an approach guarantees potential bioactivity and proper cereal seed germination. Egypt Pharm J 2023.
61. Husain S, Verma SK, Azam M, Sardar M, Haq Q, Fatma T. Antibacterial efficacy of facile cyanobacterial silver nanoparticles inferred by antioxidant mechanism. Mater Sci Engineering: C. 2021;122:111888.
62. Ameen F, Abdullah MM, Al-Homaidan AA, Al-Lohedan HA, Al-Ghanayem AA, Almansob A. Fabrication of silver nanoparticles employing the cyanobacterium Spirulina platensis and its bactericidal effect against opportunistic nosocomial pathogens of the respiratory tract. J Mol Struct. 2020;1217:128392.
63. Selvamani V. Stability studies on nanomaterials used in drugs. Characterization and biology of nanomaterials for drug delivery. Elsevier; 2019. pp. 425–44.
64. Ismail GA, El-Sheekh MM, Samy RM, Gheda SF. Antimicrobial, antioxidant, and antiviral activities of biosynthesized silver nanoparticles by phycobiliprotein crude extract of the cyanobacteria spirulina platensis and Nostoc linckia. Bionanoscience. 2021;11:355–70.
65. El-Sheekh MM, Hassan LH, Morsi HH. Assessment of the in vitro anticancer activities of cyanobacteria mediated silver oxide and gold nanoparticles in human colon CaCo-2 and cervical HeLa cells. Environ Nanatechnol Monit Manage. 2021;16:100556.
66. Acharya TR, Lee GJ, Choi EH. Influences of plasma plume length on Structural, Optical and Dye Degradation properties of citrate-stabilized silver nanoparticles synthesized by plasma-assisted reduction. Nanomaterials. 2022;12(14):2367.
67. Borkar SB, Negi M, Acharya TR, Lamichhane P, Kaushik N, Choi EH, Kaushik NK. Mitigation of T3SS-mediated virulence in waterborne pathogenic bacteria by multi-electrode cylindrical-DBD plasma-generated nitric oxide water. Chemosphere. 2024;350:140997.
68. Zhou S, An W, Gan C, Xu M. Environmental implications of bacterial-derived extracellular reactive oxygen species. Int Biodeterior Biodegrad. 2024;187:105706.
69. Joshi SG, Cooper M, Yost A, Paff M, Ercan UK, Fridman G, Friedman G, Fridman A, Brooks AD. Nonthermal dielectric-barrier discharge plasma-induced inactivation involves oxidative DNA damage and membrane lipid peroxidation in Escherichia coli. Antimicrob Agents Chemother. 2011;55(3):1053–62.
70. Dhakal OB, Dahal R, Acharya TR, Lamichhane P, Gautam S, Lama B, Kaushik NK, Choi EH, Chalise R. Effects of spark dielectric barrier discharge plasma on water sterilization and seed germination. Curr Appl Phys. 2023;54:49–58.
71. Acharya TR, Lamichhane P, Jaiswal A, Amsalu K, Hong YJ, Kaushik N, Kaushik NK, Choi EH. The potential of multicylindrical dielectric barrier discharge plasma for diesel-contaminated soil remediation and biocompatibility assessment. Environ Res. 2024;240:117398.
72. Zhang H, Zhang C, Han Q. Mechanisms of bacterial inhibition and tolerance around cold atmospheric plasma. Appl Microbiol Biotechnol. 2023;107(17):5301–16.
73. Moritz M, Geszke-Moritz M. The newest achievements in synthesis, immobilization and practical applications of antibacterial nanoparticles. Chem Eng J. 2013;228:596–613.
74. Lee SM, Song KC, Lee BS. Antibacterial activity of silver nanoparticles prepared by a chemical reduction method. Korean J Chem Eng. 2010;27:688–92.
75. Marius S, Lucian H, Marius M, Daniela P, Irina G, Romeo-Iulian O, Simona D, Viorel M. Enhanced antibacterial effect of silver nanoparticles obtained by electrochemical synthesis in poly (amide-hydroxyurethane) media. J Mater Science: Mater Med. 2011;22:789–96.
76. Zhao X, Duan C, Liang Z, Shen H. Preparation of self-assembled Ag nanoparticles for effective light-trapping in crystalline silicon solar cells. RSC Adv. 2014;4(27):13757–63.
77. Feroze N, Arshad B, Younas M, Afridi MI, Saqib S, Ayaz A. Fungal mediated synthesis of silver nanoparticles and evaluation of antibacterial activity. Microsc Res Tech. 2020;83(1):72–80.
78. El-Naggar NE-A, Hussein MH, El-Sawah AA. Bio-fabrication of silver nanoparticles by phycocyanin, characterization, in vitro anticancer activity against breast cancer cell line and in vivo cytotxicity. Sci Rep. 2017;7(1):10844.
79. Aletayeb P, Ghadam P, Mohammadi P. Green synthesis of AgCl/Ag3 PO4 nanoparticle using cyanobacteria and assessment of its antibacterial, colorimetric detection of heavy metals and antioxidant properties. IET Nanobiotechnol. 2020;14(8):707–13.
80. Karageorgou D, Zygouri P, Tsakiridis T, Hammami MA, Chalmpes N, Subrati M, Sainis I, Spyrou K, Katapodis P, Gournis D. Green Synthesis and characterization of silver nanoparticles with high antibacterial activity using cell extracts of Cyanobacterium Pseudanabaena/Limnothrix sp. Nanomaterials. 2022;12(13):2296.

Publisher's note